Alanine and glutamate catabolism ensure proper sporulation by preventing premature germination and providing energy respectively

Fengzhi Lyu, Tianyu Zhang, Dong Yang, Lei Rao*, Xiaojun Liao*

College of Food Science and Nutritional Engineering, National Engineering Research Center for Fruit and Vegetable Processing, Key Laboratory of Fruit and Vegetable Processing of Ministry of Agriculture and Rural Affairs, Beijing Key Laboratory for Food Non-Thermal Processing, China Agricultural University, Beijing, China

***Correspondence**

Lei Rao, College of Food Science and Nutritional Engineering, China Agricultural University, 100083, Beijing,China.

Email: rao.lei@cau.edu.cn

Xiaojun Liao, College of Food Science and Nutritional Engineering, China Agricultural University, 100083, Beijing,China.

Email: liaoxjun@cau.edu.cn

Abstract

Sporulation as a typical bacterial differentiation process has been studied for decades. However, two crucial aspects of sporulation, (i) the energy sources supporting the process, and (ii) the maintenance of spore dormancy throughout sporulation, are scarcely explored. Here, we reported the crucial role of RocG-mediated glutamate catabolism in regulating mother cell lysis, a critical step for successful sporulation, likely by providing energy metabolite ATP. Notably, *rocG* overexpression resulted in an excessive ATP accumulation in sporulating cells, leading to adverse effects on future spore properties, e.g. increased germination efficiency, reduced DPA content, and lowered heat resistance. Additionally, we revealed that Ald-mediated alanine metabolism decreased the typical germinant L-alanine concentration in sporulating environment, thereby preventing premature germination and maintaining spore dormancy. Our data inferred that sporulation was a highly orchestrated biological process requiring a delicate balance in diverse metabolic pathways, hence ensuring both the completion of sporulation and production of high-quality spores.

Introduction

Spores are generated by spore-forming bacteria such as the orders *Bacillales* and *Clostridiales* in response to unfavorable environmental conditions, such as nutrient limitation (1, 2). Spores are metabolically dormant and considered the most resilient living organisms due to their extreme resistance to harsh environments, and they are capable of surviving for millions of years (3-5). The process of forming spores from bacterial vegetative cells is termed sporulation. Taking the model bacterium *Bacillus subtilis* as an example, the morphological process of sporulation can be divided into several stages: asymmetric division, engulfment, spore maturation, mother cell lysis, and spore release (6, 7). Initially, as vegetative cells commit to sporulation, the earliest visible event is asymmetric division, which produces the septum, dividing the vegetative cell into a larger mother cell and a smaller forespore. Subsequently, the mother cell membrane migrates around the forespore until it is completely enclosed. This phagocytosis-like process is identified as engulfment. Concurrently, the double-membrane structure of the forespore forms, followed by cortex synthesis and spore coat assembly. Then, the forespore chromosomes become saturated with small acid-soluble proteins (SASPs), and the water within the forespore is replaced by dipicolinic acid (DPA) synthesized in the mother cell, resulting in forespore dehydration. These events culminate in the appearance of phase-bright spores. Next, mother cell lysis occurs after spore maturation, allowing the spores to be released into the environment.

Research on the morphological events of the sporulation process, as well as the underlying gene expression and molecular mechanisms, has been continued for decades (6, 8-11). However, relative few studies focus on guaranteeing proper sporulation, especially concerning the quantity and quality of spores. Proper sporulation encompasses two essential aspects. The

first is the normal progression of sporulation. Sporulation is recognized as an energy-intensive biological process (12), implying the importance of energy supply in promoting its progress. Studies have suggested that amino acid metabolism, such as glutamate and alanine catabolism, may serve as potential energy sources driving sporulation (13-15). However, the mechanisms regulating these processes during sporulation remain unclear. Secondly, proper sporulation needs the maintenance of spore dormancy throughout the process. Previous studies report that the deletion of *ylbJ*, *pdaB*, or genes encoding SpoVA protein results in premature germination, indicating the loss of dormancy maintenance ability of generated spores during sporulation (16, 17). The reasons for these types of premature germination are varied, including inappropriate activation of germination receptors, incorrect assembly of spore outer structures, and deficiencies in the SpoVA channel (16, 17). Except for these intrinsic factors, quantities of external factors such as nutrient germinants that induce germination may also exist around the generated spores. How spores maintain dormant in such a tempting environment remains a mystery to be explored. Therefore, defects in either energy supply or dormancy maintenance can lead to abnormal sporulation, adversely affecting the quantity or quality of spores produced.

Here, we reported that the RocG-mediated glutamate catabolism played a crucial role in ensuring proper sporulation, particularly by promoting mother cell lysis through providing energy support. Our research further demonstrated that overexpression of *rocG* resulted in excessively high ATP contents in sporulating cells, which adversely affected the properties of the resulting spores, e.g. elevated germination efficiency, reduced DPA content, and lowered heat resistance. Moreover, we revealed that Ald-mediated alanine catabolism decreased the concentration of typical germinant L-alanine in the sporulating environment to a certain level. This regulation effectively prevented premature germination and contributed to maintain spore dormancy

106 throughout the sporulation process.

107

108 **Results**

109

110 **Proteins involved in alanine, aspartate and glutamate metabolism show**
111 **enrichment according to proteomics analysis during sporulation of *B.***
112 ***subtilis***

113

114 In order to explore the essential metabolic pathways in *B. subtilis* sporulation,
115 Tandem Mass Tag-based (TMT) quantitative proteomics analysis was
116 conducted comparing dormant spores (DS) and sporulating vegetative cells
117 (VC) at t_0 (Figure 1A). Hierarchical clustering analysis (HCA) was employed to
118 illustrate the overall differences in proteins between the DS and VC groups
119 (Figure 1B). The HCA heatmap displayed greater differences between groups
120 than within groups, indicating significant differences in proteins between DS
121 and VC. Differentially-expressed proteins were identified based on the criteria
122 of $p < 0.05$ and fold change > 1.2 (the expression level increased by more
123 than 1.2-fold or decreased by less than 0.83-fold). 1,259 proteins with
124 decreased expression as well as 1,248 proteins with increased expression
125 were screened out in the DS group (Figure 1C). KEGG pathway enrichment
126 analysis of these differentially expressed proteins revealed the significant
127 alterations in several metabolic pathways between the DS and VC groups,
128 including alanine, aspartate and glutamate metabolism, ribosome, flagellar
129 assembly, glyoxylate and dicarboxylate metabolism, and methane metabolism
130 (Figure 1D). Of these pathways, the most significant changes were observed
131 in alanine, aspartate and glutamate metabolism, implying their close
132 association with the sporulation of *B. subtilis*. Previous studies have indicated
133 that *ald*, encoding alanine dehydrogenase Ald, and *rocG*, encoding glutamate
134 dehydrogenase RocG, are crucial regulators of alanine and glutamate
135 metabolism, respectively (14, 18). In addition, Δ*ald* and Δ*rocG* mutants have

136 shown notable defects in sporulation (14, 15). However, the deletion of *ansB*
137 gene, encoding L-aspartase important for aspartate metabolism, has no
138 significant effect on sporulation (19). Consequently, further exploration was
139 conducted in the following work to elucidate the effects of alanine and
140 glutamate metabolism on sporulation.
141
142 **Alanine and glutamate metabolism collaboratively regulate sporulation**
143 **with an additive effect**
144
145 Given that alanine and glutamate metabolism have been reported separately
146 to be involved in sporulation (14, 15, 20), we wonder if there are any potential
147 joint impacts of these two pathways on sporulation. We constructed the Δ*ald*
148 Δ*rocG* mutant and observed a significantly lower number of phase-bright
149 spores compared to the Δ*ald* or Δ*rocG* mutants (Figure 2A). This indicated
150 that the sporulation defect in the Δ*ald* Δ*rocG* mutant was more pronounced
151 than in either the Δ*ald* or Δ*rocG* mutants. This was further demonstrated by
152 examining the heat-resistant spores produced in sporulation, as the
153 percentage of the Δ*ald* and Δ*rocG* spores was 10.9% and 29.8% respectively,
154 while the Δ*ald* Δ*rocG* mutant was only 0.3% (Figure 2B). The severe
155 sporulation defect of the double mutant suggested that Ald and RocG jointly
156 regulated sporulation in an additive manner. Additionally, we observed an
157 accumulation of phase-dark forespores in the Δ*ald* Δ*rocG* mutant (Figure 2A),
158 which could be attributed to two factors: (i) premature germination due to
159 abnormal spore structure assembly or an inappropriate in-situ sporulating
160 environment (16) , or (ii) failure of spore maturation due to limited energy
161 supporting sporulation progression. We first deleted *gerAA* to investigate if
162 premature germination occurred in the Δ*ald* Δ*rocG* mutant. As shown in
163 Figure 3A, the sporulation defect of the double mutant was partially rescued,
164 with 29.7% of phase-bright spores formed in the Δ*ald* Δ*rocG* Δ*gerAA* (Δ3)
165 mutant. This result indicated that premature germination indeed existed in the

166 Δ*ald* Δ*rocG* mutant. However, the partial rescue effect suggested that
167 premature germination was not the exclusive reason for sporulation defect in
168 the Δ*ald* Δ*rocG* mutant. Therefore, the limitation of energy support remained a
169 substantial explanation for the sporulation defect phenotype observed in the
170 double mutant strain. Nonetheless, we further explored these two possibilities
171 in the following work.
172
173 **RocG-mediated glutamate metabolism, rather than Ald-mediated alanine**
174 **metabolism, is essential for ensuring both the sporulation efficiency and**
175 **the spore quality, likely through energy supply**
176
177 As the Ald and RocG mediated alanine and glutamate metabolisms were
178 proposed as potential energy sources for sporulation (14, 15), we
179 hypothesized that these two metabolic pathways contribute to energy support
180 independently. If this was true, excessive complementation of either metabolic
181 pathway should be capable of rescuing the sporulation defect observed in the
182 Δ*ald* Δ*rocG* mutant. Here, we used the Δ*ald* Δ*rocG* Δ*gerAA* (Δ3) strain to
183 exclude the premature germination effect and independently explored the
184 energy supply mechanism (Figure 3A). Based on this, *ald* and *rocG* were
185 artificially expressed separately and jointly in Δ3 under an IPTG-inducible
186 promoter. Results indicated that increasing the expression level of *ald* by
187 raising the concentration of IPTG up to 5 mM had no significant effect on the
188 quantity of phase-bright spores in the Δ3 mutant, with the sporulation
189 percentage ranging between 20% and 30% (Figure S1, Figure S2A).
190 Accordingly, these spores exhibited significant germination deficiency under
191 AGFK induction (Figure S2B, Figure 3C). However, elevating the *rocG*
192 expression level with the addition of at least 10 mM IPTG restored the
193 sporulation of the Δ3 mutant to 53.4%, similar to that of the wild-type (56.8%)
194 (Figure 3B). Furthermore, when more than 20 mM IPTG was added, the
195 germination deficiency of the Δ3 mutant spores was also recovered to the

196 level of the wild-type (Figure S2B, Figure 3C). Notably, the Δ3 mutant with
197 IPTG-induced co-expression of *ald* and *rocG* exhibited the same sporulation
198 and germination phenotypes as those with IPTG-induced sole expression of
199 *rocG* (Figure S2B, Figure 3C). Hence, in the Δ3 mutant, sole complementation
200 of RocG succeeded in rescuing the sporulation defect, unlike in the case of
201 Ald. This indicated that RocG-mediated glutamate metabolism appeared to
202 regulate sporulation by providing energy sources, whereas Ald-mediated
203 alanine metabolism may not play the same role.
204
205 To further investigate whether these two catabolic pathways are involved in
206 controlling the spore quality, mutants of transcription factors of Ald and RocG,
207 Δ*adeR* and Δ*ahrC* Δ*rocR* (15, 21), were respectively constructed to examine
208 the germination phenotype of the spores. *gerAA* was also knocked out in
209 these mutants to ensure the comparability of experimental results. The
210 deletion of transcription factors was demonstrated to reduce, rather than
211 completely eliminate, the expression of regulated genes (Figure 4B), and this
212 rescued the sporulation deficiency (Figure 4A). Interestingly, no significant
213 germination defect was observed in spores of the Δ*adeR* Δ*gerAA* mutant with
214 decreased expression of *ald* (Figure 4C). However, spores of the Δ*ahrC*
215 Δ*rocR* Δ*gerAA* mutant with low expression of *rocG* showed a remarkable
216 germination deficiency (Figure 4C). Moreover, spores of the Δ*adeR* Δ*ahrC*
217 Δ*rocR* Δ*gerAA* mutant exhibited a similar germination deficiency phenotype to
218 that of Δ*ahrC* Δ*rocR* Δ*gerAA* mutant spores (Figure 4C), indicating that the
219 expression of *rocG*, rather than *ald*, was essential for ensuring spore quality
220 with normal germination capability. Taken together, these results strongly
221 implied that RocG-mediated glutamate metabolism regulated both sporulation
222 efficiency and spore quality, probably through energy supply. As for Ald-
223 mediated alanine metabolism, its effect on sporulation was unlikely to be
224 executed by providing energy sources. Instead, it is more reasonably
225 associated with premature germination, as quantities of phase-dark spores

226 were observed in the sporulating cells of the Δ*ald* mutant (Figure 2A).

227

228 **Ald inhibits premature germination during sporulation by reducing L-**
229 **alanine content in the external environment of generating spores**

230

231 As mentioned above, the presence of phase-dark spores in the Δ*ald* mutant
232 prompted us to investigate the impact of Ald-mediated alanine metabolism on
233 premature germination. As illustrated in Figure 5A-5B, the Δ*ald* mutant
234 produced significant quantities of phase-dark spores, and the percentage of
235 phase-bright spores was only 11.5%. However, upon the deletion of *gerAA* in
236 the Δ*ald* mutant, the percentage of phase-bright spores significantly raised to
237 61.5%, approaching levels observed in the wild-type (76.5%). In addition, no
238 notable deficiency in germination was observed in Δ*ald* Δ*gerAA* spores
239 compared to the wild-type (Figure 5C). Thus, it can be concluded that the
240 absence of Ald led to sporulation defect by inducing premature germination
241 during sporulation. To identify the timing of premature germination occurrence,
242 the sporulation process of the Δ*ald* mutant was examined by time-lapse
243 microscopy. Interestingly, two models were observed: (i) forespores
244 prematurely germinated during mother cell lysis, and then were released; (ii)
245 dormant spores were released and subsequently induced to premature
246 germination (Figure 5D).

247

248 The connection between Ald and premature germination raised up an
249 intriguing speculation that the interruption of alanine metabolism may lead to
250 an over-accumulation of L-alanine, which triggers premature germination. To
251 investigate this, *ald* was artificially expressed in the Δ*ald* mutant under an
252 IPTG-inducible promoter, and the sporulation phenotype as well as the
253 environmental L-alanine content at the late sporulation phase (t_{19}) of these
254 mutants were examined. The results showed a gradual increase in the
255 percentage of phase-bright spores with elevating the expression levels of *ald*

256 (Figure 6A-6C). Notably, the expression of *ald* decreased as the concentration
257 of added IPTG increased to 1 mM, which was possibly due to the toxicity of
258 IPTG to cells (Figure 6C). In contrast, an opposite trend was observed in the
259 environmental L-alanine concentration of the Δ*ald* mutant, which reached
260 3,397.4 μM without IPTG induction, while decreased to wild-type levels of
261 145.9 μM when > 200 μM IPTG was added to elevate the *ald* expression
262 (Figure 6B). Consequently, Ald-mediated alanine metabolism was responsible
263 for reducing the L-alanine content in the external environment of spores to
264 prevent premature germination, and thus ensuring proper sporulation.
265
266 **RocG plays a crucial role in regulating both σ^K-dependent spore release**
267 **and spore properties likely by providing energy sources**
268
269 As indicated above, RocG-mediated glutamate metabolism regulated both
270 sporulation efficiency and spore quality likely through energy support. To
271 further explore the underlying mechanism, we focused on identifying the
272 specific sporulation stage interrupted by *rocG* deletion. We constructed strains
273 capable of reporting stage-specific sigma factors involved in sporulation,
274 namely σ^F, σ^E, σ^G, and σ^K, which respectively regulated polar division,
275 engulfment, spore maturation, and spore release (6, 11, 22, 23). P_{spoIIQ}, P_{spoIID},
276 P_{sspB}, and P_{gerE} promotors that was respectively recognized by σ^F, σ^E, σ^G, and
277 σ^K were fused to *gfp*. In general, the activation of a particular σ factor
278 correlates with σ-dependent GFP fluorescence, thereby visually displaying the
279 impaired sporulation stage (22). Our results demonstrated that the activation
280 patterns of σ^F and σ^E in the Δ*rocG* mutant were similar to those of the wild-
281 type (Figure S3). The activation of σ^G could be achieved in the Δ*rocG* mutant,
282 though there was a delay in the activation timepoint (Figure 7A). Remarkably,
283 σ^K-dependent GFP fluorescence in the Δ*rocG* mutant initially appeared at t_7
284 but abnormally persisted until t_{25} (Figure 7B). Since σ^K regulates cell wall lytic
285 enzymes, leading to mother cell lysis (24, 25), its fluorescence is supposed to

286 disappear with spore release. The persistence of σ^K-dependent GFP
287 fluorescence at the end of sporulation in the Δ*rocG* mutant indicated the
288 failure of mother cell lysis, a process mainly executed by the sporulation-
289 specific cell wall lytic enzymes CwlC and CwlH (24, 26). As expected, the
290 expression level of *cwlC* and *cwlH* were remarkably lower in the Δ*rocG* mutant
291 compared to those in the wild-type (Figure 7C). Taken together, the deletion of
292 *rocG* had no notable effect on the activation of sporulation-specific σ factors
293 but hindered mother cell lysis by impacting the expression of cell wall lytic
294 enzymes, resulting in an impaired spore release process (Figure 7D).
295
296 To further understand the regulating role of RocG in sporulation, *rocG* was
297 artificially expressed in the Δ*rocG* mutant under an IPTG-inducible promoter.
298 The results showed a significant increase in the percentage of released
299 spores with elevating expression levels of *rocG* (Figure 8A-8C). Moreover, the
300 addition of more than 10 μM IPTG remarkably improved the percentage of
301 spore release to the wild-type level (Figure 8A, 8C). As hypothesized
302 previously, RocG-mediated glutamate metabolism could provide energy
303 sources to drive sporulation proceeding, we then examined the ATP levels in
304 sporulating cells to verify this. Since previous research has demonstrated that
305 the ATP content of mother cells during sporulation peaked at t_1 (15, 27), we
306 examined ATP content at t_1 in the Δ*rocG* mutant with different *rocG* expression
307 levels. Accordingly, the level of ATP in the Δ*rocG* mutant increased with the
308 elevation of *rocG* expression (Figure 8D). The positive correlation between
309 the ATP level in sporulating cells (Figure 8D) and future spore release (Figure
310 8C) suggested the crucial role of energy supply in the late sporulation process,
311 particularly in mother cell lysis. Notably, the ATP content of the Δ*rocG* mutant
312 with 50 μM IPTG induction was almost double that of the wild-type (Figure 8D).
313 We then wondered if such a high level of ATP in sporulating cells could affect
314 the properties of the future spores. To test this, the spores generated under
315 different concentrations of IPTG induction were purified and examined for

316 germination phenotypes, as well as DPA content and heat resistance.
317 Interestingly, Δ*rocG* spores with 50 μM IPTG induction showed higher
318 germination efficiency (Figure 8G-8I) but significantly lower DPA content
319 (Figure 8E) as well as decreased heat resistance (Figure 8F) compared to the
320 wild-type spores. Taken together, the expression of *rocG* can indeed provide
321 energy support for sporulation, especially for mother cell lysis regulated by σ^K,
322 thus contributing to the proper sporulation process. However, overexpression
323 of *rocG* can accumulate excessive ATP in sporulating cells, which might
324 adversely affect the spore properties.
325
326 **Discussion**
327
328 Sporulation as a typical bacterial differentiation process has been extensively
329 studied for decades, and the morphological events along with the signal
330 transduction for this process are relatively well elucidated (6, 8-11). However,
331 as an energy-consuming process, the sources of energy supply and the
332 underlying regulating mechanism lack research. In addition, how the
333 generated spores maintain in dormant state during sporulation remains
334 mysterious. Here, we demonstrated that Ald-mediated alanine metabolism
335 decreased the concentration of the typical germinant L-alanine in the
336 sporulating environment to a certain level, thus avoiding premature
337 germination and maintaining spore dormancy. Moreover, we also provided
338 evidences supporting that RocG-mediated glutamate metabolism ensured
339 proper sporulation, especially mother cell lysis, by regulating ATP levels
340 during sporulation. Additionally, excessively high ATP levels during the
341 sporulation process was supposed to adversely affect the properties of the
342 produced spores, including faster germination efficiency, lower DPA content,
343 along with decreased heat resistance. Our data revealed that sporulation was
344 a highly orchestrated and exquisite biological process requiring the balance of
345 diverse metabolic pathways, e.g. alanine catabolism to eliminate surrounding

346 germinants, and glutamate metabolism providing an appropriate level of
347 energy to ensure both sporulation completion and the high quality of
348 generated spores (Figure 9).
349
350 Our finding of alanine catabolism eliminating the germinant L-alanine raises
351 another open question that which catabolic pathways or biological reactions
352 are responsible for regulating the balance of other potential germinants during
353 sporulation. Indeed, sporulation involves protein turnover, in which new
354 proteins are continuously synthesized using the amino acids derived from the
355 breakdown of pre-existing cellular protein (28, 29). Hence, substantial free
356 amino acids exist during sporulation, which could serve as potential
357 germinants. Moreover, non-sporulating cells can produce meso-
358 diaminopimelic acid (m-DAP) type muropeptides, also identified as possible
359 germinants (30). However, the mechanisms by which spores eliminate these
360 potential germinants remain unclear. Our research revealed that alanine
361 catabolism is one of the strategies employed to achieve this. While we also
362 observed that L-alanine was not completely eliminated, as 145.9 μM L-alanine
363 was still detected in the sporulating medium of the wild-type (Figure 6B). Why
364 did the presence of residual L-alanine in the environment not trigger
365 germination? One plausible explanation is that alanine racemases present in
366 the spore coat can convert the germinant L-alanine into the germination
367 inhibitor D-alanine, thereby allowing the spores to persist in dormancy (31).
368 However, whether there are alternative mechanisms preventing the residual
369 L-alanine and other germinants from triggering germination is worth exploring.
370
371 Another new finding in our study revealed that RocG-mediated glutamate
372 metabolism plays a crucial role as an energy source for sporulation. Indeed,
373 the catabolic product of glutamate, 2-oxoglutarate (2-OG), directly participates
374 in the tricarboxylic acid (TCA) cycle, showing its superior efficiency in
375 providing energy during nutrient-limited sporulation (32, 33). Concurrently,

various amino acids such as proline, ornithine, citrulline, and arginine can be converted into glutamate through the arginine degradation pathway (34), indicating its high availability in sporulating cells. These aspects give glutamate an advantage in supporting energy during sporulation compared to other amino acids. Additionally, glutamate stands out among the limited free amino acids found within diverse spores (35), further suggesting its crucial role during sporulation. In our study, we showed that ATP produced by glutamate catabolism is highly corelated with mother cell lysis regulated by the cell wall lytic enzymes CwlC and CwlH, and the interruption of this catabolism remarkably reduced the expression of these two enzymes. This finding implies that the energy derived from glutamate catabolism is crucial for the expression of genes regulating the final stage of sporulation. Moreover, we also observed that the overaccumulation of ATP in sporulating cells through glutamate catabolism adversely affected the properties of future spores. These effects may be attributed to abnormal changes in the structure assembly or molecular reservoir in the generated spores (28, 36). Actually, spores can inherit molecules from sporulating cells, such as alanine dehydrogenase and ATP, to modulate their revival capability (36). Moreover, glutamate, as a universal amino group donor in all living organisms, can serve as a carbon or nitrogen source for synthesizing other amino acids and DPA during sporulation (34, 35, 37). Additionally, the glutamate catabolic intermediate 2-OG can contribute to the synthesis of amino acids, nucleotides, and NADH (32), potentially affecting the structure construction or molecular modulation of spores. All these evidences support that glutamate is an ideal substrate for energy supply and the synthesis of new substances during sporulation, ensuring both the proper sporulation process and the quality of the spores.

404 **Methods**

405

406 **Strains and plasmids**

407

408 *B. subtilis* strains used in this study are listed Table S1. Plasmids construction
409 is listed in Table S2, and primers are described in Table S3. For gene
410 replacement strategy, primer pairs were used to amplify the flanking genomic
411 regions of the corresponding gene. PCR products and the respective
412 antibiotic resistance gene were used for Gibson assembly (NEB, USA) (38).
413 The product was used to transform *B. subtilis* PY79 to obtain the mutant allele.

414

415 **General methods**

416

417 All general methods for *B. subtilis* were carried out as described previously
418 with some modifications (15). Cultures of wild-type and mutant strains were
419 cultivated in LB medium (Difco) at 37 °C. Sporulation was carried out at 37°C
420 by suspending overnight cells (OD_{600} = 0.05) in Schaeffer's liquid medium
421 (Difco Sporulation Medium, DSM) (39). Sporulation t_0 was identified as the
422 third hour after spores suspending in DSM. The percentage of sporulation
423 was evaluated by calculating the ratio of total number of colonies forming
424 units (CFU) before and after heat treatment (80°C, 20 min) (40). The
425 percentage of phase-bright or released spores were counted based on the
426 according phase-contrast images. To ensure confidence of the data, > 800
427 cells were counted for each experiment. Spore germination with different
428 germinants was examined as described previously with some modifications
429 (15, 41). Briefly, purified spores were heat activated at 75°C for 30 min, and
430 then induced by L-Alanine (10 mM) or AGFK (2.5 mM L-Asparagine, 5 mg/mL
431 D-glucose, 5 mg/mL D-fructose, and 50 mM KCl) at 37°C, or DDA (1 mM in 10
432 mM Tris-HCl, pH 7.4) at 42°C. The germination was tested by determining the
433 DPA release as descried in the following text.

434 **Spore purification**

435

436 Matured spores were purified as described previously (15). Briefly, 22 hrs
437 DSM culture was centrifuged and washed 3 times by DDW and then kept in
438 4°C with constant agitation. The suspension was washed once a day and
439 resuspended in DDW. After 7 days, the suspension was centrifuged to collect
440 the pellet. 20% histodenz solution was used to resuspend the pellet at a ratio
441 of 400 μL per 10 mL of DSM for 30 min on ice. Aliquots (200 μL) of
442 resuspension mixture were then added on top of 900 μL 50% histodenz
443 solution, and gradient fractionation was carried out by centrifugation at 15,000
444 rpm at 4°C for 30 min. The pellet was collected and washed at least 5 times
445 by DDW. Phase contrast microscopy was then used to evaluate the purity of
446 pellet spores. Spores with >99% purity can be used for following experiments,
447 otherwise the purification steps should be carried out more than once.

448

449 **Tandem Mass Tag-based (TMT) quantitative proteomics analysis**

450

451 TMT quantitative proteomics analysis was carried out between pure dormant
452 spores (DS) and vegetative cells (VC) at sporulation t_0 by Shanghai Applied
453 Protein Technology Co., Ltd (Shanghai, China). DS and VC samples were
454 collected by centrifugation and then freeze-dried and bead-grinded using
455 FastPrep-24 (M. P. Biomedicals, LLC, USA). Samples were then extracted for
456 proteins and labeled using TMT reagent. Proteomics analysis was then
457 carried out by LC-MS/MS system with on a Q Exactive mass spectrometer
458 (Thermo Scientific) that was coupled to Easy nLC (Proxeon Biosystems, now
459 Thermo Fisher Scientific). The raw data for each sample were searched using
460 the MASCOT engine (Matrix Science, London, UK; version 2.2) embedded
461 into Proteome Discoverer 1.4 software for identification and quantitation
462 analysis. Hierarchical clustering analysis was performed using Cluster 3.0
463 (http://bonsai.hgc.jp/~mdehoon/software/cluster/software.htm) and Java

464 Treeview software (http://jtreeview.sourceforge.net). Enrichment analysis was
465 performed based on KEGG database (http://geneontology.org/). A statistical
466 analysis was performed using a t-test to determine the significance (p-value)
467 of differentially-expressed proteins. The expression level of proteins with $p <$
468 0.05 and fold change > 1.2 (the expression level increased by more than 1.2-
469 fold or decreased by less than 0.83-fold) were considered as significant
470 difference.
471
472 **DPA measurements**
473
474 DPA release was detected as described previously with some modifications
475 (42). Briefly, spore germination was induced by L-Ala, AGFK or DDA at 37°C
476 or 42°C in a 96-well plate. Spores at OD_{600} of 20, 10 mM germinants, 25 mM
477 K-Hepes buffer (pH 7.4) as well as 50 mM $TbCl_3$ were mixed in 200 μL and
478 Tb^{3+}-DPA fluorescence intensity was monitored at Ex/Em = 270/545 nm by a
479 TECAN Spark 10M microplate reader (TECAN, Switzerland). Total DPA
480 content of spores were evaluated by boiling the spores (OD_{600} of 1) for 20 min
481 and mixing the spores and 50 mM $TbCl_3$ to 200 μL in a 96-well plate. The DPA
482 standard solution was serially diluted and detected together to obtain a
483 standard curve. The detection parameters for DPA release were the same as
484 above, and the total DPA content of spores was calculated based on the
485 standard curve.
486
487 **Phase-contrast and fluorescence microscopy**
488
489 Phase-contrast and fluorescence microscopy were performed using a Nikon
490 DS-Qi2 microscope equipped with a Nikon Ph3 DL 100x/1.25 Oil phase
491 contrast objective. Both bacterial cells (500 μL) and spores (50 μL) were
492 centrifuged, and the pellets were resuspended with 5 ~ 10 μL PBSx1 and then
493 imaged. For time-lapse imaging of sporulation, Imaging System Cell Chamber

494 (AttofluorTM Cell Chamber) was used. Sporulating cells were collected by
495 centrifugation. The supernatant DSM was collected to make a gel-pad with
496 1% agarose. The collected sporulating cells were incubated on the DSM gel-
497 pad in a chamber at 37 °C. Image analysis and processing were performed by
498 ImageJ2.
499
500 **Real-Time Quantitative PCR (RT-qPCR)**
501
502 Real-time quantitative PCR (RT-qPCR) was carried out followed the protocol
503 described previously (15). RNA samples of sporulating cells (500 μL) were
504 collected from DSM by centrifugation, and then extracted by FastPure
505 Cell/Tissue Total RNA Isolation Kit V2 (Vazyme Biotech Co..Ltd). HiScript III
506 All in-one RT SuperMix for qPCR (Vazyme Biotech Co..Ltd) was used to
507 reverse transcribed RNA samples. RT-qPCR reactions were conducted with
508 PerfectStart Green qPCR SuperMix (TransGen Biotech Co., Ltd). CFX
509 Connect RealTime PCR Dection System (Bio-Rad Laboratories (Shanghai)
510 Co., Ltd.) was used to detect the fluorescence and *scr* gene was selected to
511 normalize sample data (zhou23). Each experiment was performed triplicate.
512
513 **Environmental L-alanine content assay**
514
515 Measurement of environmental L-Alanine level was performed as the
516 instruction of Amplite Fluorimetric L-Alanine Assay Kit (AAT Bioquest, Inc.).
517 DSM media of sporulating cells at sporulation t_{19} was collected from the
518 supernatant after centrifugation. The fluorescence intensity of L-Alanine in
519 DSM media was monitored by TECAN Spark 10M microplate reader (TECAN,
520 Switzerland) at Ex/Em = 540/590 nm. The standard solution of L-alanine was
521 serially diluted and detected together to obtain a standard curve, and the L-
522 Alanine content in the environment was calculated based on the standard
523 curve.

524 **ATP content assay**

525

526 Measurement of ATP content in mother cell was performed using the
527 BacTiter-Glo Microbial Cell Viability Assay (Promega). As guided by the
528 instructions, sporulating cells in DSM at sporulation t_1 were collected and
529 detected luminescence using a TECAN Spark 10M microplate reader (TECAN,
530 Switzerland). The standard solution of ATP was serially diluted and detected
531 simultaneously to obtain a standard curve, and the ATP level was calculated
532 based on the standard curve.

533

534 **Data processing**

535

536 Unless stated otherwise, each experiment was carried out at least triplicate.
537 GraphPad Prism 8 software was used for all statistical analysis, data
538 processing, and graph drawing. One-way ANOVA was performed to analyze
539 the variance and $p < 0.05$ was regarded as significance for all data statistics.

540

541 **Data availability**

542

543 The data that support the findings of this study are available from the authors
544 on reasonable request.

545

546 **Acknowledgements**

547

548 We are grateful to Dr. Bing Zhou (The Hebrew University of Jerusalem) for
549 valuable discussions and comments. This work was supported by National
550 Natural Science Foundation of China (NSFC) (grant No. 32372470), NSFC
551 (grant No. 32001658), Agricultural Research Outstanding Talents of China
552 (grant No. 13210317) awarded to Lei Rao, and 2115 Talent Development
553 Program of China Agricultural University.

Author contributions

F. L. and L. R. conceived the idea of the experiment. F. L. contributed to the acquisition and analysis of data as well as writing the draft. T. Z. contributed to the construction of mutant strains. Y. D., L. R., and X. L. contributed to revising the paper.

Competing interests

The authors declare no competing interests.

565 **References**

566

567 1. Driks A. 2002. Maximum shields: the assembly and function of the
568 bacterial spore coat. Trends Microbiol 10:251-254.
569 2. Stragier P, Losick R. 1996. Molecular genetics of sporulation in *Bacillus*
570 *subtilis*. Annu Rev Genet 30:297-41.
571 3. Nicholson WL, Munakata N, Horneck G, Melosh HJ, Setlow P. 2000.
572 Resistance of *Bacillus* endospores to extreme terrestrial and
573 extraterrestrial environments. Microbiol Mol Biol Rev 64:548-572.
574 4. Setlow P. 2006. Spores of *Bacillus subtilis*: their resistance to and
575 killing by radiation, heat and chemicals. J Appl Microbiol 101:514-525.
576 5. Vreeland RH, Rosenzweig WD, Powers DW. 2000. Isolation of a 250
577 million-year-old halotolerant bacterium from a primary salt crystal.
578 Nature 407:897-900.
579 6. Riley EP, Schwarz C, Derman AI, Lopez-Garrido J. 2020. Milestones in
580 *Bacillus subtilis* sporulation research. Microb Cell 8:1-16.
581 7. Higgins D, Dworkin J. 2012. Recent progress in *Bacillus subtilis*
582 sporulation. FEMS Microbiol Rev 36:131-148.
583 8. Tokuyasu K, Yamada E. 1959. Fine Structure of *Bacillus subtilis*: II.
584 Sporulation Progress. The Journal of Cell Biology 5:129-133.
585 9. Kawata T, Inoue T, Takagi A. 1963. Electron microscopy of spore
586 formation and germination in *Bacillus subtilis*. Japanese Journal of
587 Microbiology 7:23-41.
588 10. Piggot P, Coote J. 1976. Genetic aspects of bacterial endospore
589 formation. Bacteriological reviews 40:908-962.
590 11. Errington J. 2003. Regulation of endospore formation in *Bacillus*
591 *subtilis*. Nat Rev Microbiol 1:117-126.
592 12. Phillips Z, Strauch M. 2002. *Bacillus subtilis* sporulation and stationary
593 phase gene expression. Cell Mol Life Sci 59:392-402.
594 13. Charba J, Nakata H. 1977. Role of glutamate in the sporogenesis of

595 *Bacillus cereus*. J Bacteriol 130:242-248.
596 14. Siranosian KJ, Ireton K, Grossman AD. 1993. Alanine dehydrogenase
597 (ald) is required for normal sporulation in *Bacillus subtilis*. J Bacteriol
598 175:6789-6796.
599 15. Rao L, Zhou B, Serruya R, Moussaieff A, Sinai L, Ben-Yehuda S. 2022.
600 Glutamate catabolism during sporulation determines the success of the
601 future spore germination. iScience 25:105242.
602 16. Ramírez‐Guadiana FH, Meeske AJ, Wang X, Rodrigues CD, Rudner
603 DZ. 2017. The *Bacillus subtilis* germinant receptor GerA triggers
604 premature germination in response to morphological defects during
605 sporulation. Mol Microbiol 105:689-704.
606 17. Gao Y, Barajas-Ornelas RDC, Amon JD, Ramírez-Guadiana FH, Alon A,
607 Brock KP, Marks DS, Kruse AC, Rudner DZ. 2022. The SpoVA
608 membrane complex is required for dipicolinic acid import during
609 sporulation and export during germination. Genes Dev 36:634-646.
610 18. Belitsky BR, Sonenshein AL. 1998. Role and regulation of *Bacillus*
611 *subtilis* glutamate dehydrogenase genes. J Bacteriol 180:6298-6305.
612 19. Yoshida K, Fujita Y, Ehrlich SD. 1999. Three asparagine synthetase
613 genes of *Bacillus subtilis*. J Bacteriol 181:6081-91.
614 20. de Vries YP, Atmadja RD, Hornstra LM, de Vos WM, Abee T. 2005.
615 Influence of glutamate on growth, sporulation, and spore properties of
616 *Bacillus cereus* ATCC 14579 in defined medium. Appl Environ Microbiol
617 71:3248-3254.
618 21. Lin TH, Wei GT, Su CC, Shaw GC. 2012. AdeR, a PucR-type
619 transcription factor, activates expression of L-alanine dehydrogenase
620 and is required for sporulation of *Bacillus subtilis*. J Bacteriol 194:4995-
621 5001.
622 22. Meeske AJ, Rodrigues CD, Brady J, Lim HC, Bernhardt TG, Rudner DZ.
623 2016. High-throughput genetic screens identify a large and diverse
624 collection of new sporulation genes in *Bacillus subtilis*. PLoS Biol

625 14:e1002341.
626 23. Hilbert DW, Piggot PJ. 2004. Compartmentalization of gene expression
627 during *Bacillus subtilis* spore formation. Microbiol Mol Biol Rev 68:234-
628 262.
629 24. Nugroho FA, Yamamoto H, Kobayashi Y, Sekiguchi J. 1999.
630 Characterization of a New Sigma-K-Dependent Peptidoglycan
631 Hydrolase Gene That Plays a Role in *Bacillus subtilis* Mother Cell Lysis.
632 J Bacteriol 181:6230-6237.
633 25. Smith TJ, Foster SJ. 1995. Characterization of the involvement of two
634 compensatory autolysins in mother cell lysis during sporulation of
635 *Bacillus subtilis* 168. J Bacteriol 177:3855-3862.
636 26. Kuroda A, Asami Y, Sekiguchi J. 1993. Molecular cloning of a
637 sporulation-specific cell wall hydrolase gene of *Bacillus subtilis*. J
638 Bacteriol 175:6260-6268.
639 27. Updegrove TB, Harke J, Anantharaman V, Yang J, Gopalan N, Wu D,
640 Piszczek G, Stevenson DM, Amador-Noguez D, Wang JD. 2021.
641 Reformulation of an extant ATPase active site to mimic ancestral
642 GTPase activity reveals a nucleotide base requirement for function.
643 elife 10:e65845.
644 28. Kornberg A, Spudich JA, Nelson DL, Deutscher MP. 1968. Origin of
645 proteins in sporulation. Annu Rev Biochem 37:51-78.
646 29. Sekar V, Hageman JH. 1987. Protein turnover and proteolysis during
647 sporulation of *Bacillus subtilis*. Folia Microbiol 32:465-480.
648 30. Dworkin J, Shah IM. 2010. Exit from dormancy in microbial organisms.
649 Nature Reviews Microbiology 8:890-896.
650 31. Yasuda Y, Kanda K, Nishioka S, Tanimoto Y, Kato C, Saito A, Fukuchi S,
651 Nakanishi Y, Tochikubo K. 1993. Regulation of L-alanine-initiated
652 germination of *Bacillus subtilis* spores by alanine racemase. Amino
653 Acids 4:89-99.
654 32. Huergo LF, Dixon R. 2015. The emergence of 2-oxoglutarate as a

655 master regulator metabolite. Microbiol Mol Biol Rev 79:419-435.
656 33. Gunka K, Commichau FM. 2012. Control of glutamate homeostasis in
657 *Bacillus subtilis*: a complex interplay between ammonium assimilation,
658 glutamate biosynthesis and degradation. Mol Microbiol 85:213-224.
659 34. Manabe K, Kageyama Y, Morimoto T, Ozawa T, Sawada K, Endo K,
660 Tohata M, Ara K, Ozaki K, Ogasawara N. 2011. Combined Effect of
661 Improved Cell Yield and Increased Specific Productivity Enhances
662 Recombinant Enzyme Production in Genome-Reduced *Bacillus subtilis*
663 Strain MGB874. Appl Environ Microbiol 77:8370-8381.
664 35. Nelson DL, Kornberg A. 1970. Biochemical Studies of Bacterial
665 Sporulation and Germination: XVIII. FREE AMINO ACIDS IN SPORES.
666 J Biol Chem 245:1128-1136.
667 36. Mutlu A, Trauth S, Ziesack M, Nagler K, Bergeest J-P, Rohr K, Becker
668 N, Höfer T, Bischofs IB. 2018. Phenotypic memory in *Bacillus subtilis*
669 links dormancy entry and exit by a spore quantity-quality tradeoff.
670 Nature Communications 9:69.
671 37. Gundlach J, Commichau FM, Stülke J. 2018. Perspective of ions and
672 messengers: an intricate link between potassium, glutamate, and cyclic
673 di-AMP. Curr Genet 64:191-195.
674 38. Guérout-Fleury A-M, Frandsen N, Stragier P. 1996. Plasmids for
675 ectopic integration in *Bacillus subtilis*. Gene 180:57-61.
676 39. Harwood CR, Cutting SM. 1990. Molecular biological methods for
677 *Bacillus*. Chichester ; New York : Wiley.
678 40. Zhou B, Semanjski M, Orlovetskie N, Bhattacharya S, Alon S, Argaman
679 L, Jarrous N, Zhang Y, Macek B, Sinai L, Ben-Yehuda S. 2019.
680 Arginine dephosphorylation propels spore germination in bacteria. Proc
681 Natl Acad Sci USA 116:14228-14237.
682 41. Vepachedu VR, Setlow P. 2007. Role of SpoVA proteins in release of
683 dipicolinic acid during germination of *Bacillus subtilis* spores triggered
684 by dodecylamine or lysozyme. J Bacteriol 189:1565-1572.

42. Yi X, Setlow P. 2010. Studies of the commitment step in the germination of spores of *Bacillus* species. J Bacteriol 192:3424-3433.

689 **Figure legends**

690

691 **Figure 1.** TMT quantitative proteomic analysis. (A) Proteins were compared
692 between dormant spores (DS) and vegetative cells (VC) of at the onset of
693 sporulation (t_0); (B) Heatmap of differential expressed proteins in DS samples
694 were grouped using Hierarchical Cluster Analysis. Each line represented a
695 protein, with fold change (FC) > 1.2 and $p < 0.05$ (T-test) as the screening
696 criteria. The proteins with significantly decreased expression were marked in
697 blue, the proteins with significantly increased expression were in red, the
698 proteins without quantitative information were in gray; (C) The volcano map of
699 proteins in DS group was drawn based on FC and the p-value of T test. The
700 proteins with significantly decreased (FC < 0.83, $p < 0.05$) and increased
701 (FC > 1.2, $p < 0.05$) expression were marked in blue and red, respectively,
702 and the non-differentiated proteins were in gray; (D) The enrichment map (Top
703 20) of KEGG pathway enrichment analysis of differentially expressed proteins
704 in the DS group by Fisher's exact test. The color of the bubble represents the
705 significance of the enriched KEGG pathway, and the color gradient represents
706 the size of the p-value (-log10), and the closer to red, the smaller the p-value.
707 The size of the bubble represents the amount of differential protein.

708

709 **Figure 2.** Alanine and glutamate metabolism collaboratively regulate
710 sporulation with an additive effect. (A) Representative phase-contrast images
711 of sporulating cells at the late sporulation stage t_{19}. *B. subtilis* PY79 (wt), YZ11
712 (Δ*ald*), YZ19 (Δ*rocG*), YZ12 (Δ*ald* Δ*rocG*), and YZ13 (Δ*ald* Δ*rocG*, *amyE::ald-*
713 *rocG*) strains were induced to sporulate in DSM at 37°C for 22 hrs and
714 followed by microscopy. Red arrowheads point to premature germinated
715 spores. Scale bar, 2 μm; (B) The percentage of sporulation of the strains
716 described in (A). Data are presented as the percentage of total number of
717 colonies forming units (CFU) before and after heat treatment (80°C, 20 min).
718 Shown is a representative experiment out of three independent biological

719 repeats.

720

721 **Figure 3.** RocG-mediated glutamate metabolism is essential for ensuring the
722 sporulation efficiency. (A) Representative phase-contrast images of
723 sporulating cells at the late sporulation stage t_{19}. *B. subtilis* PY79 (wt), YZ22
724 (Δ*ald* Δ*rocG* Δ*gerAA*), YZ24 (Δ*ald* Δ*rocG* Δ*gerAA, amyE::P*$_{IPTG}$*-rocG*), YZ25
725 (Δ*ald* Δ*rocG* Δ*gerAA, amyE::P*$_{IPTG}$*-ald*), and YZ26 (Δ*ald* Δ*rocG* Δ*gerAA,*
726 *amyE::P*$_{IPTG}$*-rocG-ald*) strains were induced to sporulate in DSM at 37°C for
727 22 hrs and followed by microscopy. 50 μM IPTG was added to the YZ24,
728 YZ25 and YZ26 cultures at the sporulation t_0 to induce corresponding gene
729 expression. Scale bar, 2 μm; (B) Quantification of the experiment described in
730 (A). Data are presented as percentages of the number of the phase-bright
731 spores and all sporulating cells in the same image (n ≥ 800 for each strain);
732 (C) AGFK-induced germination of spores collected in (A). Spores of wt, as
733 well as YZ24, YZ25, and YZ26 strains with 50 μM IPTG induction, were
734 purified and incubated with AGFK (10 mM) to trigger germination. DPA
735 release was measured by detecting the relative fluorescence units (RFU) of
736 Tb^{3+}-DPA. Shown is a representative experiment out of three independent
737 biological repeats.

738

739 **Figure 4.** The expression of *rocG* during sporulation is crucial to ensure the
740 quality of correspondingly generated spores. (A) Representative phase-
741 contrast images of sporulating cells at the late sporulation stage t_{19}. *B. subtilis*
742 PY79 (wt), YZ81 (Δ*adeR* Δ*gerAA*), YZ23 (Δ*ahrC* Δ*rocR* Δ*gerAA*), and YZ90
743 (Δ*adeR* Δ*ahrC* Δ*rocR* Δ*gerAA*) strains were induced to sporulate in DSM at
744 37°C for 22 hrs and followed by microscopy. Scale bar, 2 μm; (B) Expression
745 of the *ald* gene in wt, YZ11 (Δ*ald*) and YZ81 strains, and *rocG* gene in wt,
746 YZ19 (Δ*rocG*), and YZ23 strains. Sporulating cells were collected at t_0 and
747 detected as described in Methods; (C) AGFK-induced germination of spores

748 collected in (A). Spores of wt, YZ81, YZ23, and YZ90 strains were purified
749 and incubated with AGFK (10 mM) to trigger germination. DPA release was
750 measured by detecting the RFU of Tb^{3+}-DPA. Shown is a representative
751 experiment out of three independent biological repeats.
752
753 **Figure 5.** The absence of Ald induces premature germination during
754 sporulation. (A) Representative phase-contrast images of sporulating cells at
755 the late sporulation stage t_{19}. *B. subtilis* PY79 (wt), YZ11 (Δ*ald*), and YZ21
756 (Δ*ald* Δ*gerAA*) strains were induced to sporulate in DSM at 37°C for 22 hrs
757 and followed by microscopy. Red arrowheads point to premature germinated
758 spores. Scale bar, 2 μm; (B) Quantification of the experiment described in (A).
759 Data are presented as percentages of the number of the phase-bright spores
760 and all sporulating cells in the same image (n ≥ 800 for each strain); (C)
761 AGFK-induced germination of spores collected in (A). Spores of wt, YZ11, and
762 YZ21 strains were purified and incubated with AGFK (10 mM) to trigger
763 germination. DPA release was measured by detecting the RFU of Tb^{3+}-DPA.
764 Shown is a representative experiment out of three independent biological
765 repeats; (D) Models of the premature germination in the Δ*ald* mutant. YZ11
766 strain was induced to sporulate in DSM at 37°C. After 14 hrs of incubation,
767 sporulating cells were collected on an exhausted DSM gel-pad as described
768 in Methods, and followed by time-lapse microscopy at a 10 min interval.
769
770 **Figure 6.** Ald-mediated alanine metabolism regulates L-alanine content in the
771 external environment of generated spores. (A) Representative phase-contrast
772 images of sporulating cells at the late sporulation stage t_{19}. YZ31 (Δ*ald,*
773 *amyE::*P_{IPTG}*-ald*) strains were induced to sporulate in DSM at 37°C for 22 hrs
774 and followed by microscopy. 0-1000 μM IPTG was added at the sporulation t_0
775 to induce *ald* expression. Scale bar, 2 μm; (B) The percentage of phase-bright
776 spores as well as the environmental L-alanine content of the wt and YZ31
777 strains at the late sporulation stage t_{19}. The percentage of phase-bright spores

778 are presented as ratio of the number of the phase-bright spores and all
779 sporulating cells in the same image (n ≥ 800 for each strain); The
780 environmental L-alanine content was detected as described in Methods; (C)
781 Expression of the *ald* gene in YZ31 strains with different IPTG induction.
782 Sporulating cells were collected 10 min after IPTG addition and detected as
783 described in Methods. Shown is a representative experiment out of three
784 independent biological repeats.
785
786 **Figure 7.** Cytological sporulation assay reveals the impaired sporulation stage
787 of Δ*rocG* mutants. (A-B) Representative phase contrast and the indicated
788 fluorescent images of wt and YZ19 (Δ*rocG*) cells harboring two transcriptional
789 fusions, σ^G and σ^K, at sporulation t_4, t_7, and t_{25}. Scale bar, 2 μm; (C)
790 Expression of the *cwlC* and *cwlH* gene in wt and YZ19 strains. Sporulating
791 cells were collected at t_7 and detected as described in Methods. Shown is a
792 representative experiment out of three independent biological repeats. (D)
793 Models of the sporulation defect in the Δ*rocG* mutants.
794
795 **Figure 8.** RocG regulates both mother cell lysis and spore properties. (A)
796 Representative phase-contrast images of sporulating cells at the late
797 sporulation stage t_{19}. *B. subtilis* PY79 (wt), YZ19 (Δ*rocG*) and YZ32 (Δ*rocG,*
798 *amyE::P$_{IPTG}$-rocG*) strains were induced to sporulate in DSM at 37°C for 22
799 hrs and followed by microscopy. 0-50 μM IPTG was added to YZ32 at the
800 sporulation t_0 to induce *rocG* expression. Scale bar, 2 μm; (B) Expression of
801 the *rocG* gene in strains indicated in (A). Sporulating cells were collected 30
802 min after IPTG addition and detected as described in Methods; (C)
803 Quantification of released spores produced by strains indicated in (A). Data
804 are presented as percentages of the number of the released spores and all
805 sporulating cells in the same image (n ≥ 800 for each strain); (D) ATP levels in
806 strains indicated in (A). Sporulating culture was collected at t_1 and analyzed
807 for ATP level as described in Methods; (E) DPA content in spores of wt and

808 YZ32 with different IPTG induction. Spores were purified and boiling for 20
809 min. DPA content was measured by detecting the RFU of Tb^{3+}-DPA; (F) Heat
810 resistance of spores collected in (E). Data are presented as the percentage of
811 total number of CFU before and after heat treatment (90°C, 10 min); (G-I)
812 Germination phenotypes of spores collected in (E). Spores were purified and
813 incubated with (G) L-alanine (10 mM), (H) AGFK (10 mM), and (I) DDA (10
814 mM) to trigger germination. DPA release was measured by detecting the RFU
815 of Tb^{3+}-DPA. Shown is a representative experiment out of three independent
816 biological repeats.
817
818 **Figure 9.** The crucial roles of alanine and glutamate catabolism in ensuring
819 proper sporulation.

Figure 1

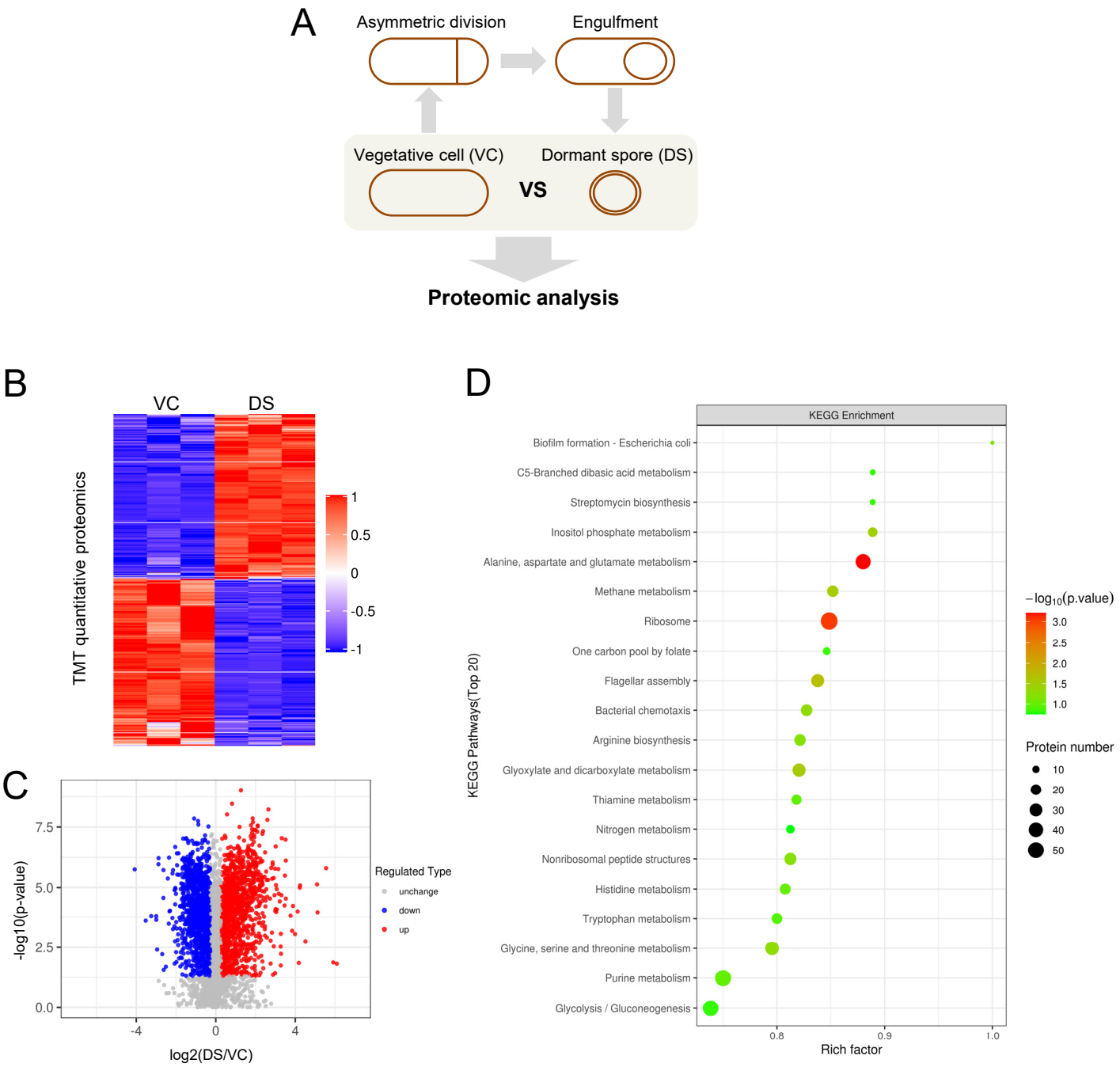
A
Asymmetric division
Engulfment
Vegetative cell (VC)
Dormant spore (DS)
VS
Proteomic analysis
B
VC
DS
TMT quantitative proteomics
1
0.5
0
-0.5
-1
C
-log10(p-value)
log2(DS/VC)
Regulated Type
unchange
down
up
D
KEGG Enrichment
KEGG Pathways(Top 20)
Biofilm formation - Escherichia coli
C5-Branched dibasic acid metabolism
Streptomycin biosynthesis
Inositol phosphate metabolism
Alanine, aspartate and glutamate metabolism
Methane metabolism
Ribosome
One carbon pool by folate
Flagellar assembly
Bacterial chemotaxis
Arginine biosynthesis
Glyoxylate and dicarboxylate metabolism
Thiamine metabolism
Nitrogen metabolism
Nonribosomal peptide structures
Histidine metabolism
Tryptophan metabolism
Glycine, serine and threonine metabolism
Purine metabolism
Glycolysis / Gluconeogenesis
Rich factor
−log10(p.value)
Protein number

Figure 2

A

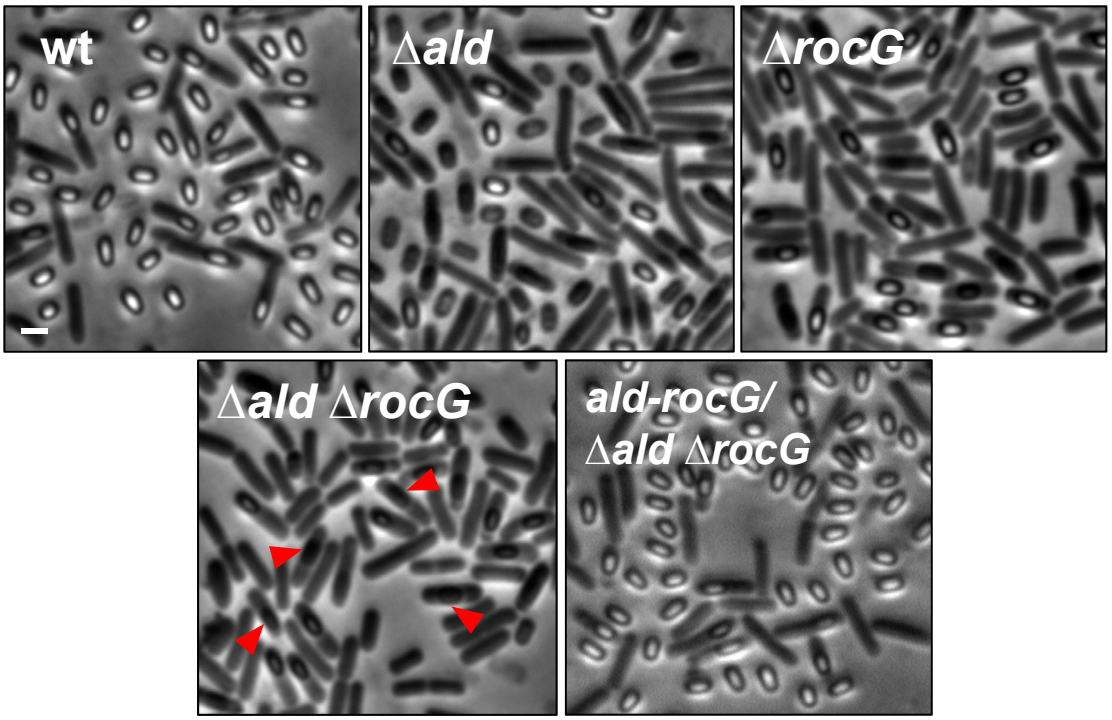
wt
Δald
ΔrocG
Δald ΔrocG
ald-rocG/
Δald ΔrocG

B

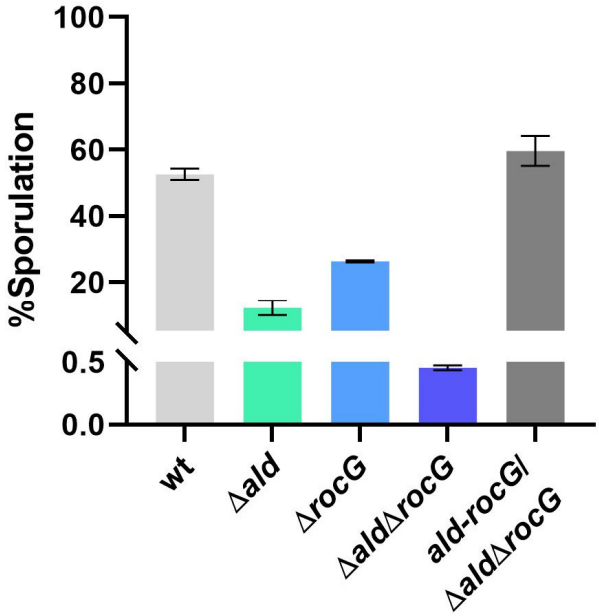
%Sporulation
100
80
60
40
20
0.5
0.0
wt
Δald
ΔrocG
ΔaldΔrocG
ald-rocG/
ΔaldΔrocG

Figure 3

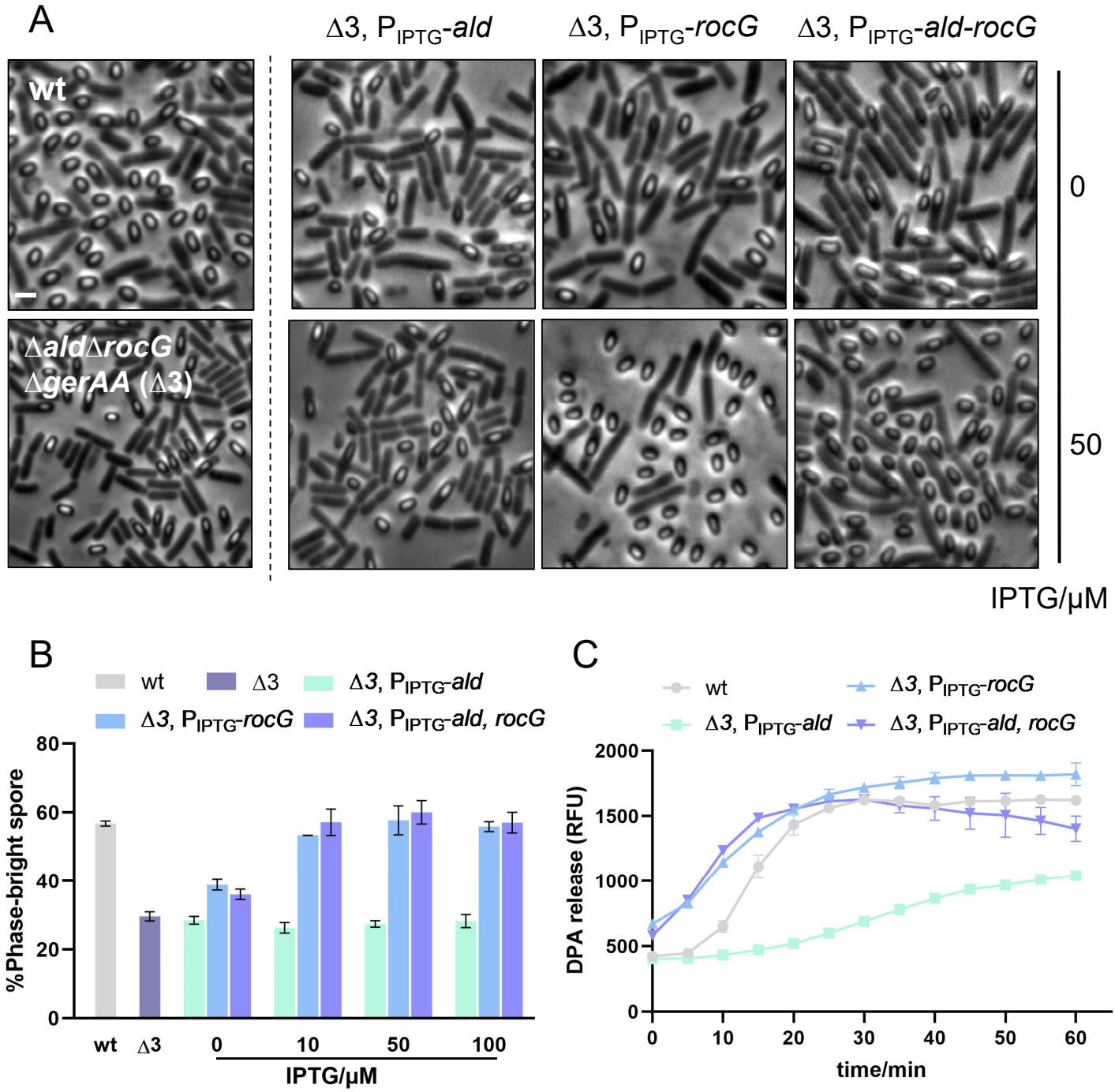
A
Δ3, P_IPTG-ald
Δ3, P_IPTG-rocG
Δ3, P_IPTG-ald-rocG
wt
ΔaldΔrocG
ΔgerAA (Δ3)
0
50
IPTG/μM
B
wt
Δ3
Δ3, P_IPTG-ald
Δ3, P_IPTG-rocG
Δ3, P_IPTG-ald, rocG
%Phase-bright spore
80
60
40
20
0
wt
Δ3
0
10
50
100
IPTG/μM
C
wt
Δ3, P_IPTG-rocG
Δ3, P_IPTG-ald
Δ3, P_IPTG-ald, rocG
DPA release (RFU)
2000
1500
1000
500
0
0
10
20
30
40
50
60
time/min

Figure 4

A

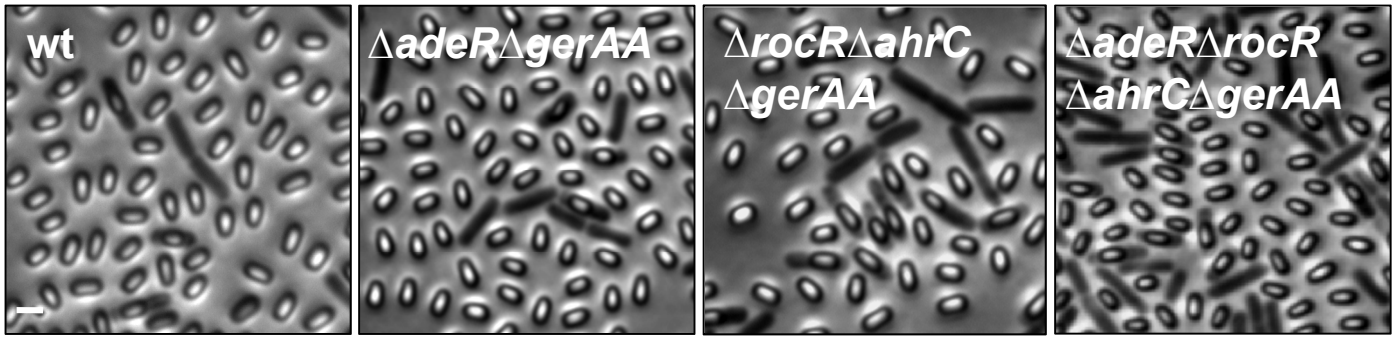
wt
ΔadeRΔgerAA
ΔrocRΔahrC
ΔgerAA
ΔadeRΔrocR
ΔahrCΔgerAA

B

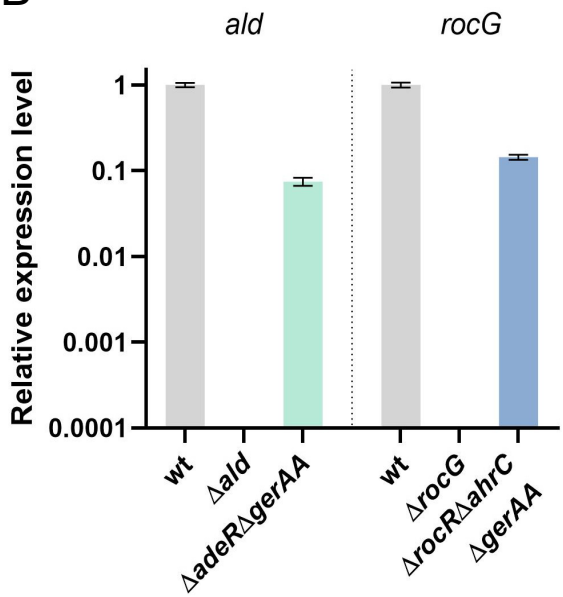
ald
rocG
Relative expression level
1
0.1
0.01
0.001
0.0001
wt
Δald
ΔadeRΔgerAA
wt
ΔrocG
ΔrocRΔahrC
ΔgerAA

C

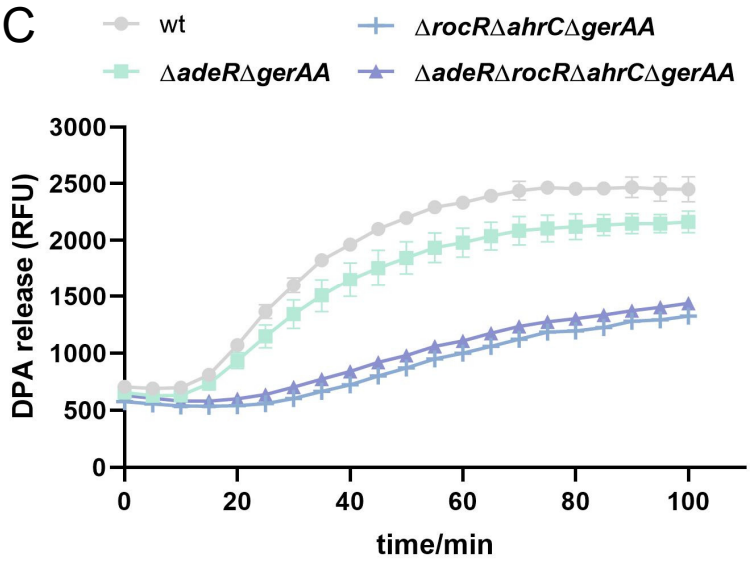
wt
ΔrocRΔahrCΔgerAA
ΔadeRΔgerAA
ΔadeRΔrocRΔahrCΔgerAA
DPA release (RFU)
3000
2500
2000
1500
1000
500
0
0
20
40
60
80
100
time/min

Figure 5

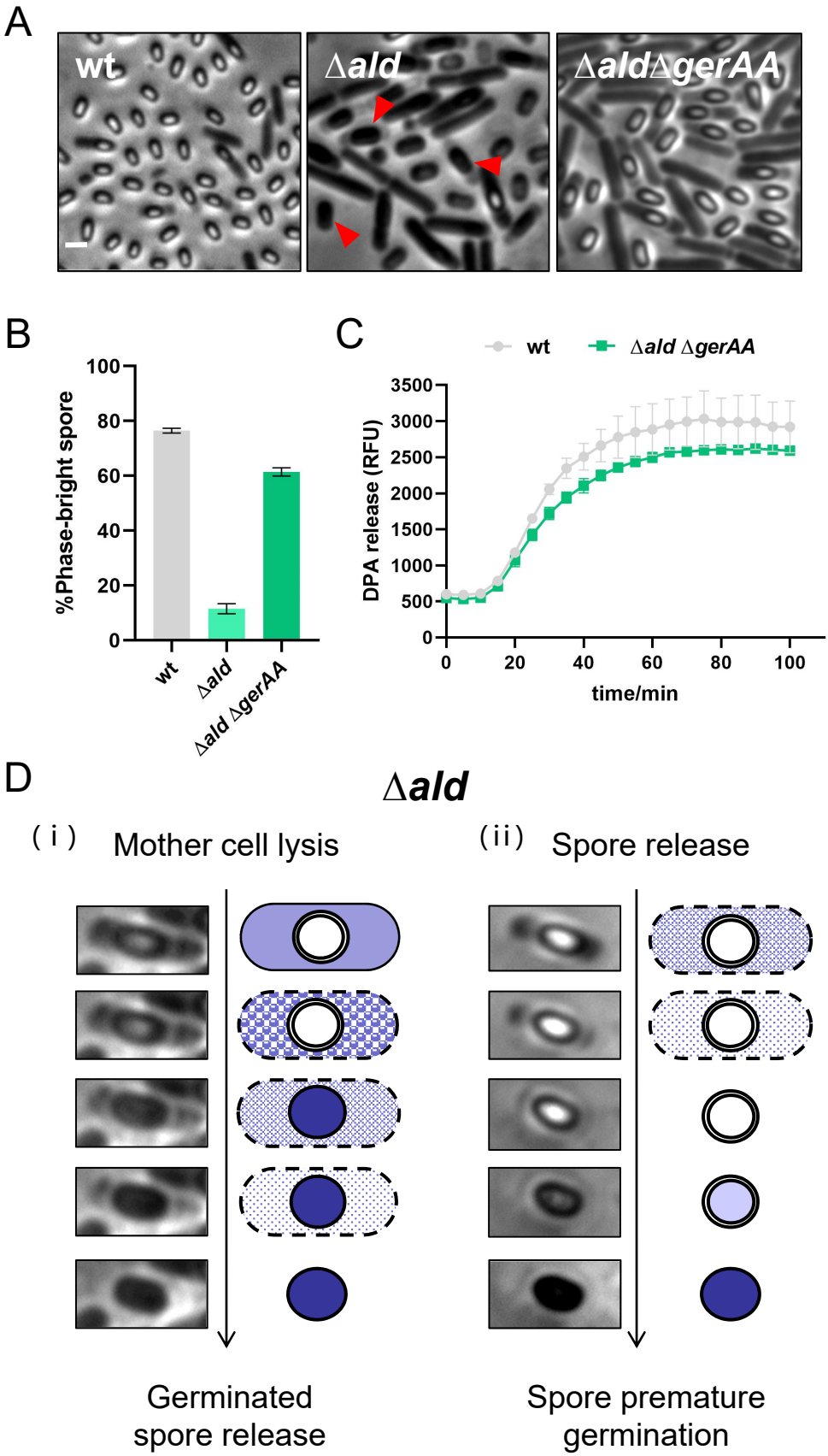
A
wt
Δald
ΔaldΔgerAA
B
%Phase-bright spore
100
80
60
40
20
0
wt
Δald
Δald ΔgerAA
C
wt
Δald ΔgerAA
DPA release (RFU)
3500
3000
2500
2000
1500
1000
500
0
0
20
40
60
80
100
time/min
D
Δald
(i)
Mother cell lysis
(ii)
Spore release
Germinated
spore release
Spore premature
germination

Figure 6

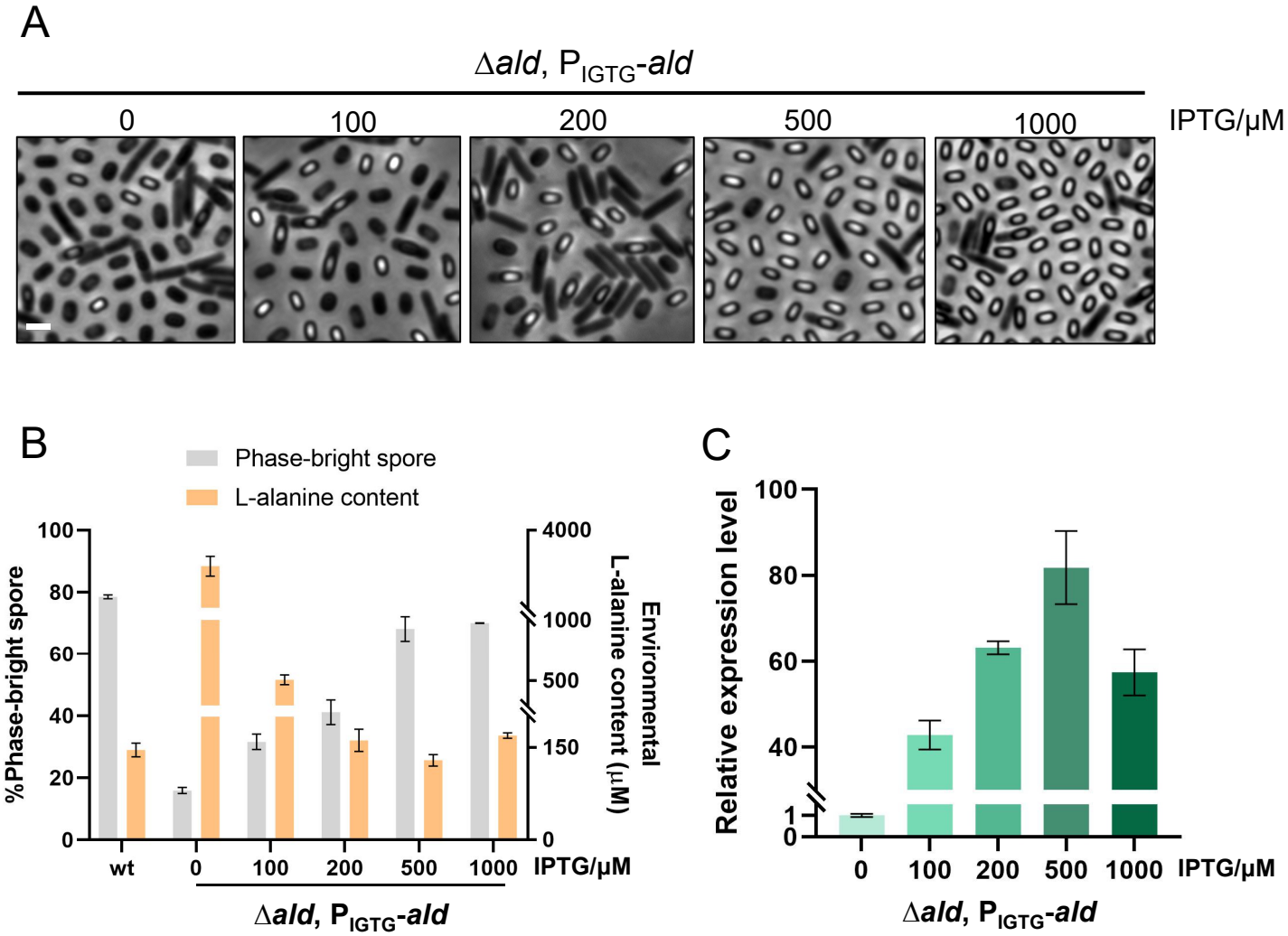
A
Δald, P_IGTG-ald
0
100
200
500
1000
IPTG/μM
B
Phase-bright spore
L-alanine content
%Phase-bright spore
Environmental L-alanine content (μM)
100
80
60
40
20
0
4000
1000
500
150
0
wt
0
100
200
500
1000
IPTG/μM
Δald, P_IGTG-ald
C
Relative expression level
100
80
60
40
1
0
0
100
200
500
1000
IPTG/μM
Δald, P_IGTG-ald

Figure 7

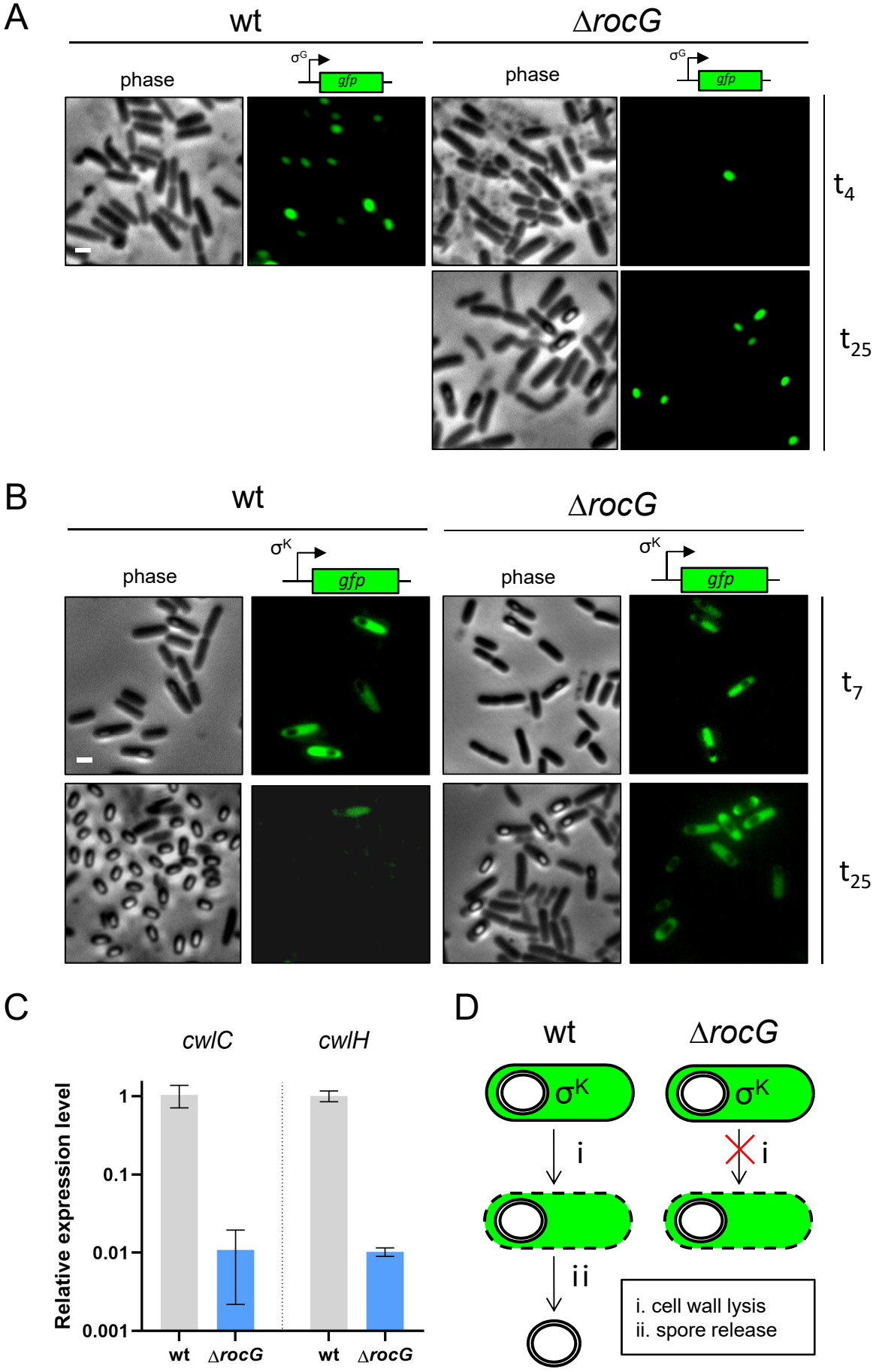
A
wt
ΔrocG
phase
σG
gfp
phase
σG
gfp
t4
t25
B
wt
ΔrocG
phase
σK
gfp
phase
σK
gfp
t7
t25
C
cwlC
cwlH
Relative expression level
1
0.1
0.01
0.001
wt
ΔrocG
wt
ΔrocG
D
wt
ΔrocG
σK
σK
i
i
ii
i. cell wall lysis
ii. spore release

Figure 8

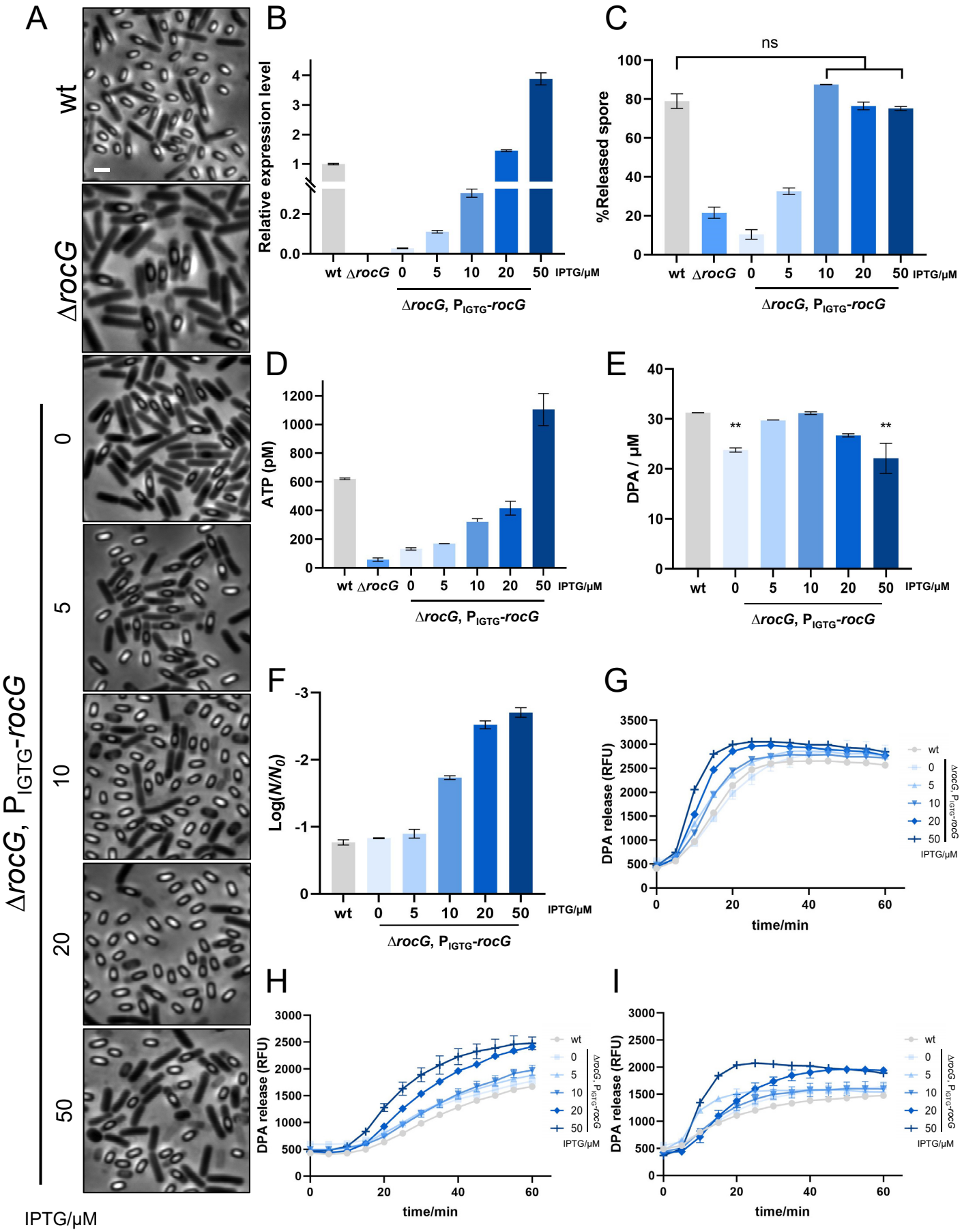
A
wt
ΔrocG
ΔrocG, PIGTG-rocG
0
5
10
20
50
IPTG/μM
B
Relative expression level
wt ΔrocG 0 5 10 20 50 IPTG/μM
ΔrocG, PIGTG-rocG
C
ns
%Released spore
wt ΔrocG 0 5 10 20 50 IPTG/μM
ΔrocG, PIGTG-rocG
D
ATP (pM)
wt ΔrocG 0 5 10 20 50 IPTG/μM
ΔrocG, PIGTG-rocG
E
DPA / μM
**
**
wt 0 5 10 20 50 IPTG/μM
ΔrocG, PIGTG-rocG
F
Log(N/N0)
wt 0 5 10 20 50 IPTG/μM
ΔrocG, PIGTG-rocG
G
DPA release (RFU)
time/min
wt
0
5
10
20
50
ΔrocG, PIGTG-rocG
IPTG/μM
H
DPA release (RFU)
time/min
I
DPA release (RFU)
time/min

Figure 9

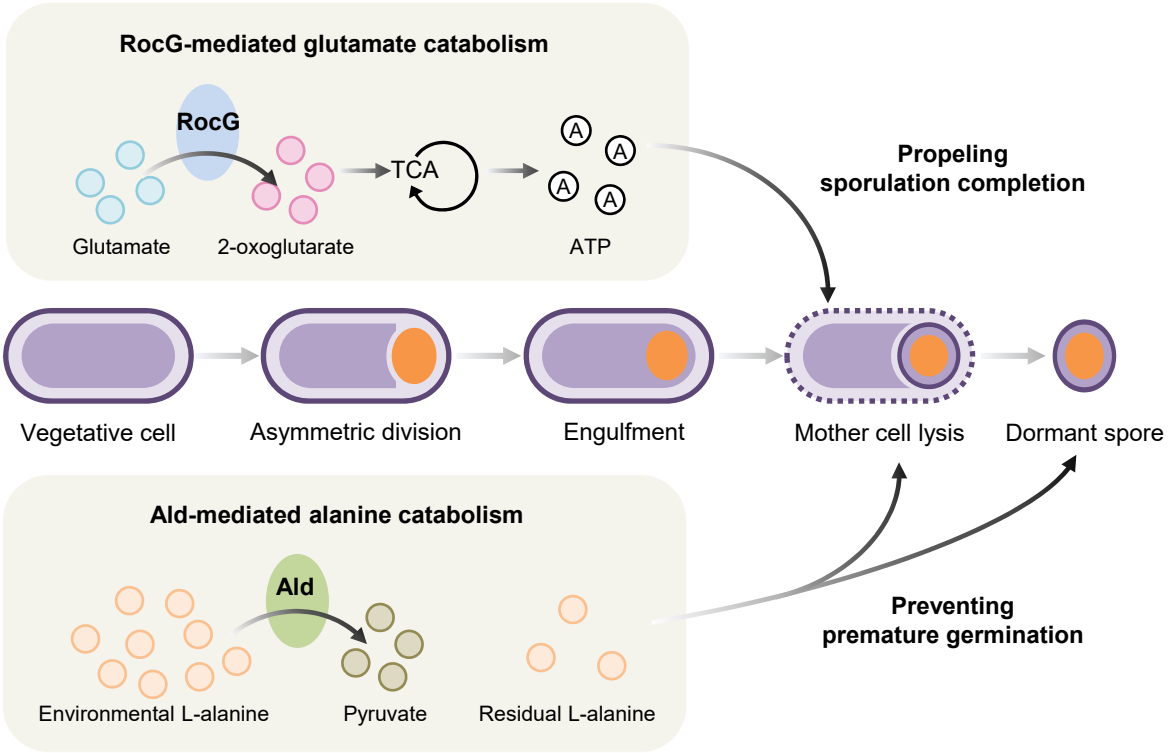
RocG-mediated glutamate catabolism
RocG
TCA
A
A
A
A
Glutamate
2-oxoglutarate
ATP
Propeling
sporulation completion
Vegetative cell
Asymmetric division
Engulfment
Mother cell lysis
Dormant spore
Ald-mediated alanine catabolism
Ald
Environmental L-alanine
Pyruvate
Residual L-alanine
Preventing
premature germination